Submitted to small NANO MICRO

DOI: 10.1002/smll.((please add manuscript number))

Destruction and control of *Toxoplasma gondii* tachyzoites using gold nanosphere/antibody conjugates

*Dakrong Pissuwan, Stella M. Valenzuela, Catherine M. Miller, Murray C. Killingsworth, Michael B. Cortie**

[*] Prof. M. B. Cortie, Ms. D. Pissuwan
Institute for Nanoscale Technology
University of Technology Sydney
P.O. Box 123 Broadway, Sydney, NSW 2007, Australia
Fax: (+61)-2-9514-2208
E-mail:Michael.cortie@uts.edu.au
Dr. S. M. Valenzuela
Department of Molecular and Bioscience
University of Technology Sydney
P.O. Box 123 Broadway, Sydney, NSW 2007, Australia
Dr. C.M. Miller
Institute for the Biotechnology of Infectious Disease
University of Technology Sydney
P.O. Box 123 Broadway, Sydney, NSW 2007, Australia
Dr. M. C. Killingsworth
Sydney South West Pathology Service
Locked Bag 7090
Liverpool BC, NSW, 1871, Australia
[**] This work was supported by the University of Technology Sydney. We thank Dr. Brian Reedy and Mr Michael Lees for technical support.

Supporting Information is available on the WWW under http://www.small-journal.com or from the author.

Keywords: gold nanoparticles, *Toxoplasma gondii*, hyperthermal therapy, antibody-functionalization

Gold nanoparticles are of interest for experimental photothermal therapies because they are biocompatible, can be functionalized with an antibody, and will strongly absorb light from suitably tuned lasers.[1-8] These attributes can be exploited to heat up and destroy specific cells to which nanoparticles have been attached. To date, most interest in using gold nanoparticles in this way has been directed at the treatment of cancer. However, we have recently extended the paradigm to attach gold nanorods to a parasitic protozoan, the infectious extracellular tachyzoite form of *Toxoplasma gondii*.[8] There are, however, some problematic issues associated with the use of nanorods, such as their positive surface charge. In the present work we show that the targeting and destruction of *Toxoplasma gondii* may be more simply achieved with simple antibody-functionalized gold nanospheres,. These aggregate on binding to the protozoan target with two unexpected but useful side-effects: a red-shift of the peak optical extinction of the gold and an inhibition of the infectivity of the tachyzoites.

Our work builds on the extensive interest in using gold nanoparticles for various biomedical applications such as biosensing,[9] imaging,[10-12] gene and drug delivery[13,14] and photothermal therapeutics.[1-4,8,12] While the chemical nobility of gold nanoparticles is valued in these applications, their plasmon resonance with light may, at times, be an additional useful factor. The peak wavelength and intensity of this resonance is dependent on the shape, size and environment of the particle. Any light absorbed is released as heat. This phenomenon of 'plasmonic heating' may be exploited to generate a localized increase in temperature in the vicinity of targeted cells in the body. A limitation of conventional photodynamic technologies is the relatively low levels of heat that can be generated at a target site,[15] however capture cross-sections of gold nanoparticles for photons can be four to five orders of magnitude greater than those of photothermal dyes.[11] We have previously reviewed the field[1] but there has been progress since then in regard to targeting of cancers,[4,5] bacteria[6] and macrophages.[7,16]

Toxoplasma gondii (*T. gondii*) is associated with the disease toxoplasmosis. The parasite is common in warm-blooded animals, including humans. Infection is generally asymptomatic in immunocompetent individuals but toxoplasmosis is likely to occur in humans with immunodeficient conditions,[17] with serious consequences. The organism has a complex life-cycle but it is sufficient to note here that acute infection is characterized by the proliferation of its motile, tachyzoite form. Tachyzoites rapidly invade and replicate themselves inside cells of the host organism. Lysing of the host cell frees the tachyzoites which spread via the bloodstream, invade new cells and initiate replication again. [18,19]

The tachyzoites can be most readily targeted with a nanoparticle-based therapy whilst they are in the extracellular medium. Gold nanospheres are a desirable platform because they are readily synthesized and conveniently conjugated with antibodies, however, gold nanorods or nanoshells have the advantage that their plasmon resonances can be tuned into the 'tissue window', the range of wavelengths at which human tissue is most transparent.[20] Although not widely known, the peak absorption of simple nanospheres can also be tuned into the tissue window, by exploiting the aggregation of multiple nanospheres that occurs as they attach to a target cell.[21] This insight unites the facile conjugation capabilities of nanospheres and the optically tunable properties of the more complex shapes into a single, readily applied, technological platform.

Gold nanospheres of approximately 20 nm diameter ('Au') were conjugated to an antibody specific to *T. gondii* ('anti-*T.g.*') to produce a gold/antibody conjugate ('Au/anti-*T.g.*') (Figure S1 of Supporting Information). Observation of cells by confocal microscopy showed fluorescent staining around the surface of tachyzoites that had been labelled with Au/anti-*T.g.* (Figure 1a). This result implied that the conjugated particles had bound to tachyzoites. A positive control, obtained by labeling anti-*T.g*. to tachyzoites followed with a secondary goat anti-mouse FITC antibody, showed a similar pattern of fluorescence (Figure 1b). No

fluorescent staining was observed in the negative control sample of tachyzoites stained with gold nanosphere/bovine serum albumin conjugates (Au/BSA) (Figure 1c) indicating that the gold nanospheres functionalized with non-specific protein or antibody did not bind to the target cells. As expected, the tachyzoites stained with only secondary FITC antibodies (Figure 1d) or with Au alone (Figure 1e) did not show any fluorescent staining. Additionally, we checked whether Au/anti-*T.g.* would bind to a non-specific target cell, U937 (Figure 1f). It did not. The attachment of Au/anti-*T.g.* to the tachyzoites was also confirmed using transmission electron microscope (TEM) imaging (Figure 2). Consideration of the TEM image and of the optical properties measured by spectrometry indicated that there were of the order of 3000 to 3500 gold nanospheres per tachyzoite.

The next step was to investigate the effect of the plasmonic heating on the tachyzoites. Two concentrations (~6.2×10^{10} and ~10.6×10^{10} nanospheres/dose respectively) of Au/anti-*T.g.* were incubated with the tachyzoites for 30 minutes. The labeled tachyzoites were then irradiated for 10 minutes at 514 nm to give a total laser dose into the samples of 600 J/cm^3. Non-labeled tachyzoites and tachyzoites incubated in the presence of Au only were also irradiated. The percentage of dead non-labeled tachyzoites after irradiation was 15.0 ± 5.9%, similar to the case for non-irradiated tachyzoites (13.3 ± 2.8%). These results indicated that laser irradiation alone did not have any adverse affect on the tachyzoites. Conversely, tachyzoites which had been labeled with Au/anti-*T.g.* at the higher concentration were preferentially destroyed after irradiation, with the death rate increasing to 26.0 ± 4.2%. However, there was no significant increase in the death rate (16.6 ± 3.2%) at the lower concentration of Au/anti-*T.g.* These results imply that there was a selective attachment of Au/anti-*T.g.* to the surface of the tachyzoites but at this comparatively low laser flux, a higher concentration of gold nanoparticles is required to destroy the targeted cells. Incubation of tachyzoites with Au only at the same two concentrations as for Au/anti-*T.g.* resulted in 11.8 ±

2.7 % and 18.9 ± 3.5% death rates respectively following irradiation. It seems that naked gold also attaches to tachyzoites during incubation, but to a lesser extent than Au/anti-*T.g.*

From the preceding experiments it was concluded that, at a given laser dose, the death rate of tachyzoites could be increased by increasing the concentration of nanospheres available for attachment. This was true of both Au/anti-*T.g.* and Au alone. Next we investigated the effect of laser dose at a fixed concentration of gold. There was no significant photothermal destruction of tachyzoites observed in the absence of Au/anti-*T.g.*, and in this case the number of dead tachyzoites did not increase even when the laser dose was increased from 900 to 2100 J/cm^3. In contrast, tachyzoites incubated with Au/anti-*T.g.* showed 24.0 ± 4.6% and 43.4 ± 8.7% death rates at 1560 and 2100 J/cm^3 respectively, compared with only 19.2 ± 4.1% dead tachyzoites at 900 J/cm^3. These results showed that the death rate of labeled tachyzoites increased at laser doses of ~1500 J/cm^3 or above, but that 900 J/cm^3 or below was insufficient to cause appreciable death.

As a further control, we investigated whether Au/BSA would bind to tachyzoites. In this case, an irradiation of 1800 J/cm^3 caused a cell death rate of 13.5 ± 3.6%. This was very similar to control samples (non-labeled tachyzoites with and without a laser at 13.4 ± 4.1% and 14.9 ± 3.7% death rate respectively, Figure 3). It is evident that Au/BSA did not attach to the tachyzoites. However, there was a significant increase in the death rate of tachyzoites labeled with Au/anti-*T.g.* and then irradiated at either 1560 J/cm^3 (24.0 ±4.6%) or 1800 J/cm^3 (24.4 ± 2.3%).

We also investigated the effect of Au/anti-*T.g.* on the infectivity of *T. gondii* into mammalian host cells (in this case CHO-K1 cells). Attachment of *T. gondii* tachyzoites to the host membrane is the first step of the invasion process after which the tachyzoites penetrate into the host cells. The percentage of CHO-K1 cells infected by non-labeled tachyzoites was 38.2 ± 6.1%. A similar percentage was also found in the sample of CHO-K1 cells incubated

with tachyzoites that had been pre-incubated with Au only (40.7 ± 12.6%). Evidently the presence of the naked gold nanospheres had no effect on the subsequent infectivity of the tachyzoites. However, pre-incubation of tachyzoites with Au-sphere/anti-*T.g.* was found to reduce the infectivity rate of the tachyzoites, with the percentage of infected cells dropping to 19.1 ± 3.4%. This was found to be significantly different to those cells exposed to either non-labeled tachyzoites or tachyzoites labeled with naked gold ($P<0.05$, Tukey's test). However, the percentage of CHO-K1 cells infected by tachyzoites was also inhibited when they were incubated with anti-*T.g.* alone (concentration of antibody about 1.4x higher than for the Au-sphere/anti-*T.g*) and was 24.8 ± 2.1%. This supports observations in the literature that anti-*T.g.* alone can inhibit the ability of the tachyzoites to infect the host cells.[22,23] The difference in infectivity between tachyzoites labeled with Au/anti-*T.g.* and those labeled with anti-*T.g.* alone was not statistically significant. Similar results were obtained with gold nanorods of 39.5 ± 0.5 nm length and 20.0 ± 0.1 nm width to which anti-*T.g.* had been conjugated. In this case the infectivity rate decreased from 38.2 ± 6.1% to 24.9± 3.4%. As expected, pre-incubation of *T. gondii* tachyzoites with gold nanorods alone showed the normal level of infectivity rate at 49.0 ± 5.8% (Figure S2, Supporting Information).

We observed that tachyzoites incubated with the Au/anti-*T.g.* were likely to stick to one another, however there was no clumping in other treatments, Figure 4. Since the tachyzoites are normally visibly motile, it is not unreasonable to speculate that this would have some effect on their infectivity. In addition, aggregation of the gold nanoparticles themselves (Figure 2) has a beneficial effect because it red-shifts their peak optical extinction towards wavelengths at which human tissue is more transparent, Figure 5 and Supporting Information (Figure S3), thereby alleviating the main disadvantage of using gold nanospheres (as opposed to more complex shapes) in a photothermal context. Furthermore, the aggregation-induced

red-shift will considerably enhance the optical contrast between isolated and targeted particles.

In summary, we have identified the potential use of gold nanospheres in a photothermal therapy to kill *Toxoplasma gondii*, a protozoan parasite. The gold nanoparticle/antibody conjugates have the additional useful effect of inhibiting the infectivity of the parasitic organism into host cells. These phenomena provide exciting new possibilities for the application of gold nanoparticles in the treatment of diseases caused by pathogenic parasites.

Experimental Section

Preparation of gold nanoparticles: Gold nanospheres were prepared by the standard citrate-reduction method and were then conjugated to anti-*T. gondii* 30 KDa antibody by following a method in the literature.[24] It is probable that the binding interaction between the protein and gold nanoparticles is electrostatic in nature.[25] The optical extinction spectrum of the conjugated particles is shown in Figure S1 of the Supporting Information.

Cell preparation: Extracellular tachyzoites were prepared by growing *T. gondii* (RH strain) in host African green monkey kidney (Vero) cells. Free tachyzoites were harvested after spontaneous lysis of Vero cells 3 to 4 days after infection of a fresh monolayer of Vero cells with tachyzoites. The gold nanosphere-antibody conjugates were then attached to the tachyzoites by incubation in vitro for 30 minutes. Tachyzoites were washed twice to remove unbound nanosphere-antibody conjugates followed by incubation with secondary antibody, goat anti-mouse labelled with fluorescein isothiocyanate (FITC) to confirm the presence of the gold conjugate. Non-specific control cells (U937, a human macrophage cell) were also treated in the same manner. The average initial percentage of dead extracellular tachyzoites after harvesting from a lysed monolayer of host cells was found to be ~15% for all

experiments presented in this paper. This number of dead tachyzoites is comparable with other reports of in vitro culturing of *T. gondii* using Vero host cells.[26] Part of the reason for the number of dead tachyzoites is the difficulty of synchronizing the precise timing between lysis of infected host cells and the subsequent use of the released tachyzoites to infect fresh host cell monolayers.[27]

Infectivity assay: The effect of Au/anti-*T.g.* on the infectivity of tachyzoites was determined by pre-incubating motile tachyzoites with Au/anti-*T.g.* for 30 min and then incubating them with CHO-K1 cells at a tachyzoite to host ratio of 5:1 for 1 hour at 37^{o}C under 5% CO_2. The monolayers of CHO-K1 cells were washed thoroughly to remove non-attached tachyzoites. After washing, cells were fixed with 4% paraformaldehyde in PBS for 25 minutes and washed twice with PBS following with cold acetone fixing for 1 minute and washed with PBS again. The cells on coverslips were then incubated with PBS plus 1% BSA for 15 minutes and washed twice with PBS followed by incubation with anti *T. gondii* 30 kDa antibody at a dilution of 1:40 for 30 minutes. Cells were washed four times with PBS and then incubated again with goat anti-mouse IgG 2^{o}abFITC at a dilution of 1:80 for 30 minutes. The percentage of CHO-K1 cells with attached *T. gondii* tachyzoites in each treatment was then determined by counting. It was assumed that attachment would necessarily be followed by infection. Protein analyses indicated that about $1.4x10^{13}$ antibody molecules/dose were applied in the form of conjugates with the gold nanospheres in each treatment of the *T. gondii* tachyzoites whereas $2.0x10^{13}$ antibody molecules/dose were applied when the tachyzoites were incubated with anti-*T.g.* alone. The number of antibody molecules conjugated with the gold nanorods was similar at $2.2x10^{13}$ molecules per dose.

Laser irradiation: Samples of 100 μL were placed in a clear glass container and then irradiated using an unfocused laser of 514 nm wavelength (Innova 70 argon laser) for ten minutes while being stirred with a magnetic stirrer. The power of the laser was varied and

measured over the interval 100 to 350 mW, and we have reported the dose as J/cm^3 (divide by 600 seconds to get W/cm^3). The viability of the tachyzoites was determined after each treatment by staining with SYTOX green dye (nucleic acid stain dye) and examination with the fluorescent mode of a confocal microscope.

Transmission electron microscopy: The solutions of tachyzoites with and without gold-antibody conjugates were fixed with 2.5% glutaraldehyde in 0.1 M sodium cacodylate buffer pH 7.4 for 4 hours for transmission electron microscopy with 120 nm thick sections. The number of gold nanospheres per cell was estimated by counting the number of gold nanoparticles (NPs) from four TEM images (mean = ~82 particles per cell) and multiplying by the number of microtome slices. The estimated number of slices was calculated by dividing the size of the cell (~5μm) by the slice thickness of the TEM samples (120 nm) and was approximately 42. The number of gold nanoparticles per cell was estimated by calculation from a standardised measurement of optical properties as shown in the Supporting Information (Figure S4).

Optical properties of aggregated gold nanoparticles: The optical properties of aggregations of gold nanoparticles were simulated using the DDSCAT computer program of Draine and Flatau[28]. A dipole volume of ~1 nm^3 was used, which is sufficiently small to give convergence for these conditions.

[1] D. Pissuwan, S.M. Valenzuela, M.B. Cortie, *Trends Biotechnol.* **2006**, 24, 62-67
[2] L.R. Hirsch, R.J. Stafford, J.A. Bankson, S.R. Sershen, B. Rivera, R.E. Price, J.D. Hazle, N.J. Halas, J.L. West, *Proc. Natl. Acad. Sci.* **2003**, 100, 13549-13554.
[3] D.P. O'Neal, L.R. Hirsch, N.J. Halas, J.D. Payne, J.L. West, *Cancer Lett.* **2004**, 209, 171-176.
[4] I.H. El-Sayed, X. Huang, M.A. El-Sayed, *Cancer Lett.* . **2006**, 239, 129-135.
[5] D. Lapotko, E. Lukianova, O. Aleinikova, A. Oraevsky, *Cancer Lett.* **2006**, 239, 36-45
[6] V.P. Zharov, K.E. Mercer, E.N. Galitovskaya, M.S. Smeltzer, *Biophys. J.* **2006**, 90, 619-627.
[7] D. Pissuwan, S.M. Valenzuela, M.C. Killingsworth, X.D. Xu, M.B. Cortie, *J. Nanoparticle Res.* **2007**, 9, 1109-1124
[8] D. Pissuwan, S. Valenzuela, C.M. Miller, M.B. Cortie, *Nano Lett.* **2007**, 7, 3808-3812.
[9] R. Elghanian, J.J. Storhoff, R.C. Mucic, R.L. Letsinger, C.A. Mirkin, *Science*. **1997**, 277, 1078-1081.
[10] V.P. Zharov, E.I. Galanzha, E.V. Shashkov, N.G. Khlebtsov, V.V. Tuchin, *Opt. Lett.* **2006**, 31, 3623-3625.
[11] C.e.a. Loo, *Technol Cancer Res*. **2004**, T 3, 33-40.
[12] X. Huang, I.H. El-Sayed, W. Qian, M.A. El-Sayed, *J. Am. Chem. Soc.* **2006**, 128, 2115-2120.
[13] H. Takahashi, Y. Niidome, S. Yamada, *Chem. Commun.* **2005**, 2247-2249
[14] G.F. Paciotti, L. Myer, D. Weinreich, D. Goia, N. Pavel, R.E. McLaughlin, L. Tamarkin, *Drug Delivery*. **2004**, 11, 169-183.
[15] F.A. Jolesz, K. Hynynen, *Cancer J.* **2002**, 8, S100–S112.
[16] D. Pissuwan, C.H. Cortie, S. Valenzuela, M.B. Cortie, *Gold Bull.* **2007**, 40, 121-129.
[17] J. Alibertie, *Nat. Rev. Imm.* **2005**, 5, 162-170.
[18] A. Tenter, A.R. Heckeroth, L.M. Weiss, *Int. J. Parasitology*. **2000**, 30, 1217-1258.
[19] J.G. Montoya, O. Liesenfeld, *The Lancet*. **2004**, 363, 1965-1976.
[20] C.R. Simpson, M. Kohl, M. Essenpreis, M. Copey, *Phys. Med. Biol.* **1998**, 43, 2465–2478.
[21] V.P. Zharov, E.N. Galitovskaya, C. Johnson, T. Kelly, *Lasers Surg. Med.* **2005**, 37, 219-226.
[22] J. Grimwood, J.E. Smith, *Experimental Parasitology*. **1992**, 74, 106-111.
[23] F. Velge-Roussel, I. Dimier-Poisson, D. Buzon-Gater, D. Bout, *Parasitology*. **2001**, 123, 225-233.
[24] J.W. Slot, H.J. Geuze, *Eur. J. Cell Biol.* **1985**, 38, 87-93.
[25] S.H. Brewer, W.R. Glomm, M.C. Johnson, M.K. Knag, S. Franzen, *Langmuir*. **2005**, 21, 9303-9307.
[26] R. Evans, J.M.W. Chatterton, D. Ashburn, A.W.L. Joss, D.O. Ho-Yen, *Euro J. Clin. Microbiol. Infect. Dis.* **1999**, 18, 879-884.
[27] D.B. Woodmansee, *J. Parasitol.* **2003**, 89, 895-898.
[28] B.T. Draine, P.J. Flatau, *J. Opt. Soc. Am. A.* **1994**, 11, 1491-1499.

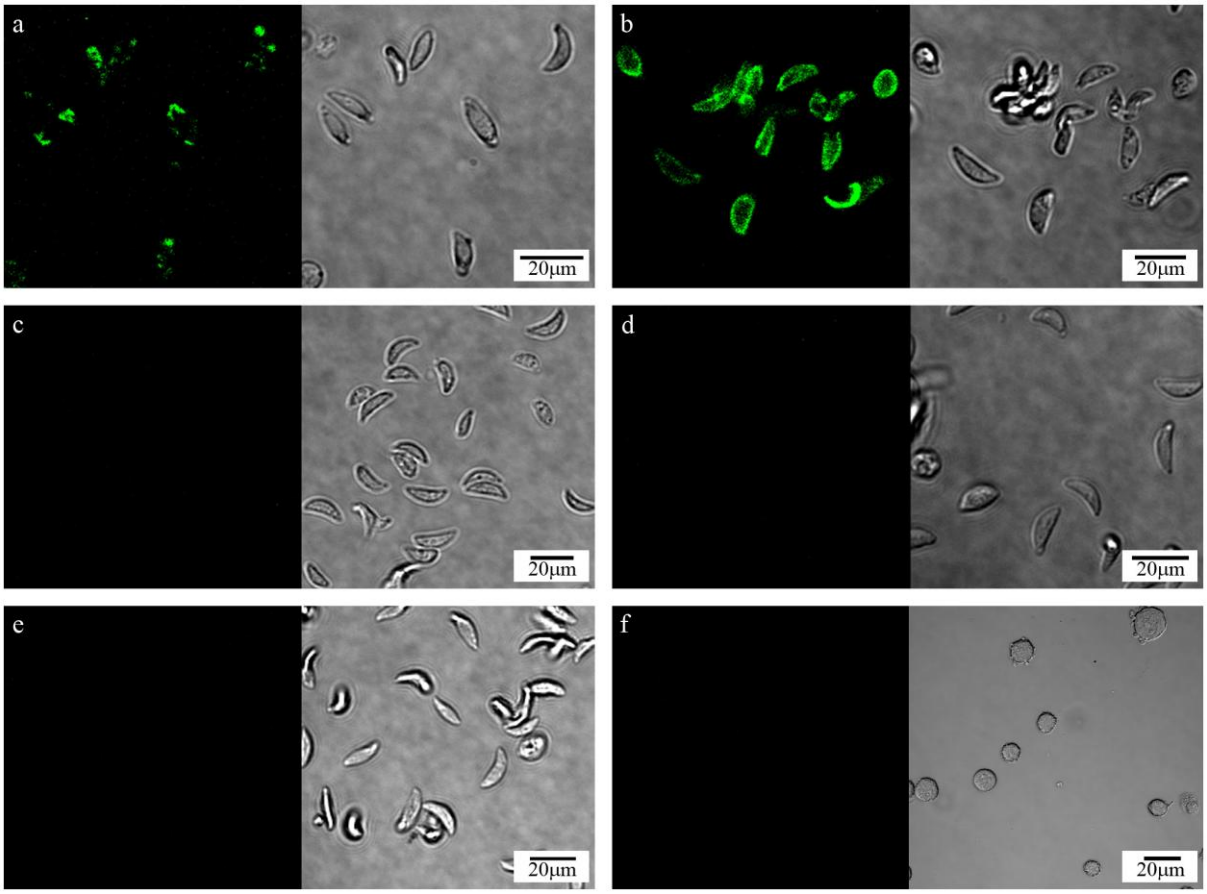

Figure 1. Fluorescence (left) and transmission (right) images of *T. gondii* tachyzoites and non-specific cells (U937) (a) *T. gondii* tachyzoites incubated with gold anti-*T. gondii* conjugates followed by incubation with goat anti-mouse IgG secondary-FITC antibody (2^{o}abFITC). (b) *T. gondii* tachyzoites incubated with anti-*T. gondii* antibody, then incubated with 2^{o}abFITC. (c) *T. gondii* tachyzoites incubated with gold-BSA conjugates then exposed to 2^{o}abFITC. (d) *T. gondii* tachyzoites exposed to 2^{o}abFITC only. (e) *T. gondii* tachyzoites incubated with non-conjugated gold nanospheres followed with 2^{o}abFITC and (f) Non-specific cells (U937) incubated with gold-anti *T. gondii* conjugates followed by exposure with 2^{o}abFITC.

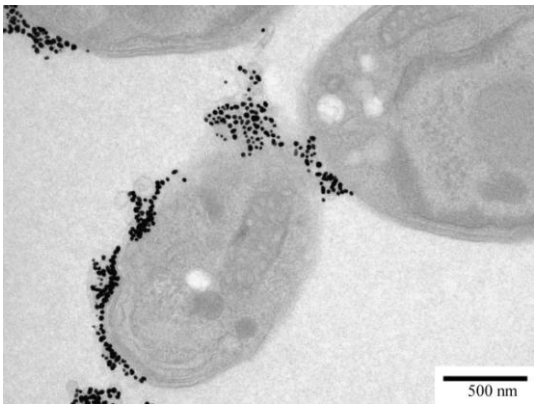

Figure 2. Transmission electron microscope image of tachyzoites of *Toxoplasma gondii* to which gold-anti *T. gondii* conjugates have become attached.

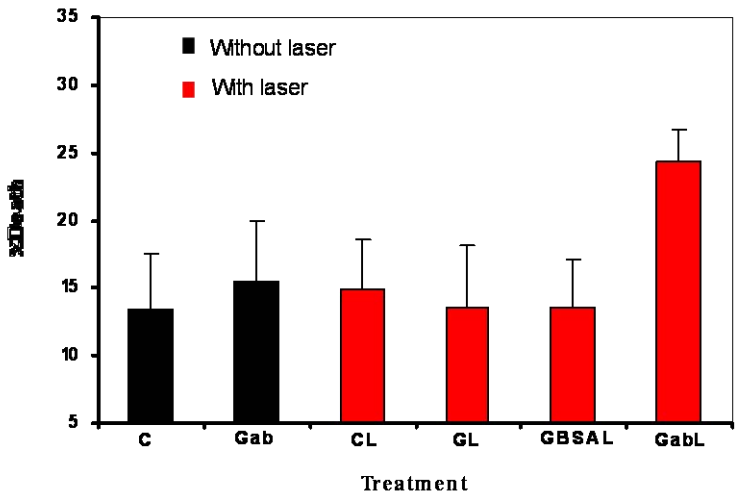

Figure 3. The percentage of cell death of *T. gondii* tachyzoites with and without exposure to the laser under different conditions. The power of laser was 1800 J/cm^3 (from 10 minutes exposure at 514 nm) and the concentration of gold nanoparticles per tachyzoite was 6.2X10^{10} NPs/dose). Key:

C= *T. gondii* tachyzoites only without laser irradiation

Gab= *T. gondii* tachyzoites incubated with gold-anti *T. gondii* conjugates without laser irradiation

CL= *T. gondii* tachyzoites only and irradiated with laser

GL= *T. gondii* tachyzoites incubated with naked gold and irradiated with laser

GBSAL= *T. gondii* tachyzoites incubated with gold-BSA conjugates and irradiated with laser

GabL= *T. gondii* tachyzoites incubated with gold-anti *T. gondii* conjugates and irradiated with laser

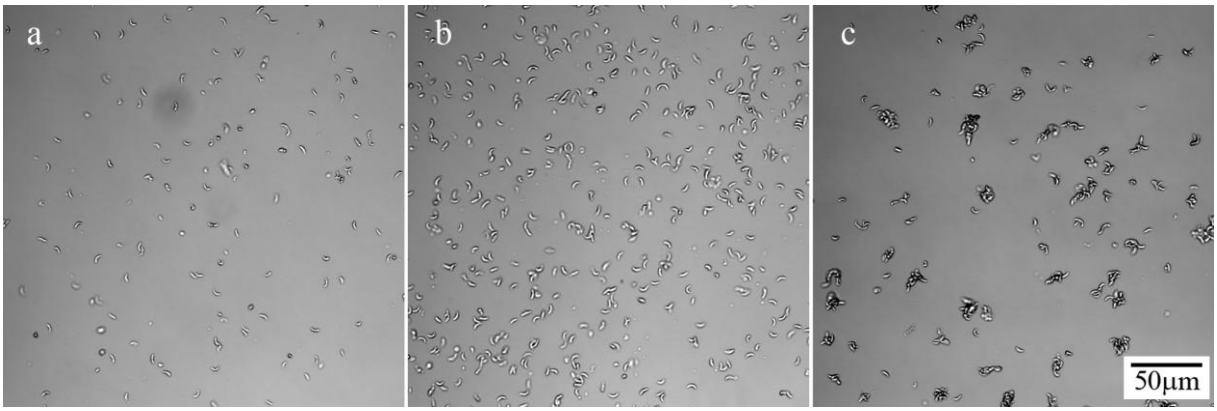

Figure 4. The distribution of tachyzoites after incubation with different solutions for 30 minutes. (a) Tachyzoites incubated with PBS buffer, (b) tachyzoites incubated with PBS plus 1%BSA, and (c) tachyzoites incubated with gold-antibody conjugates. Tachyzoites incubated with gold-antibody conjugates showed significantly clumping of cells when compared with others.

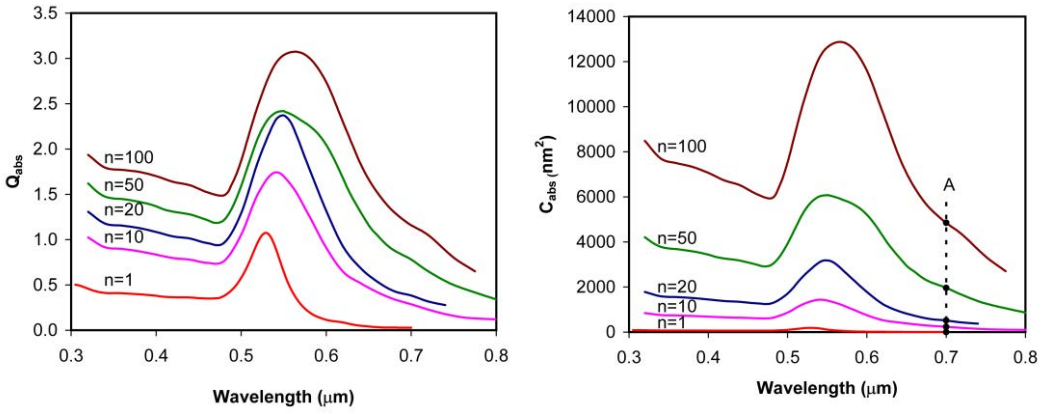

(a) (b)

Figure 5. Calculated optical extinction efficiencies of aggregations of between 1 and 100 nanospheres of 15 nm diameter in water, with a 2 nm interparticle gap. The extinction peak is broadened and red-shifted by their aggregation, and significant plasmonic heating now becomes possible in the 'tissue window'. (a) Extinction efficiencies. (b) Extinction cross-sections. Note the increased absorption cross-section along line A, for example, (n = the number of aggregated Au nanospheres)

The protozoan parasite *Toxoplasma gondii* can be selectively targeted and photothermally destroyed by gold nanosphere /antibody conjugates. The optical response of the nanospheres within the 'tissue window' is shifted and enhanced by aggregation. Attachment of the conjugates alone, even without the plasmonic heating, has the useful effect of lowering the infectivity of the organism.

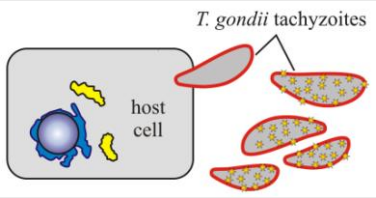

Nanoparticle targeting of tachyzoites

Dakrong Pissuwan, Stella M. Valenzuela, Catherine M. Miller, Murray C. Killingsworth, Michael B. Cortie* ____**Page No. – Page No.**

Destruction and control of *Toxoplasma gondii* tachyzoites using gold nanoparticle/antibody conjugates

Submitted to small NANO MICRO

Supporting Information:

Destruction and control of *Toxoplasma gondii* tachyzoites using nanoparticle/antibody conjugates

Dakrong Pissuwan, Stella M. Valenzuela, Catherine M. Miller, Murray C. Killingsworth, Michael B. Cortie

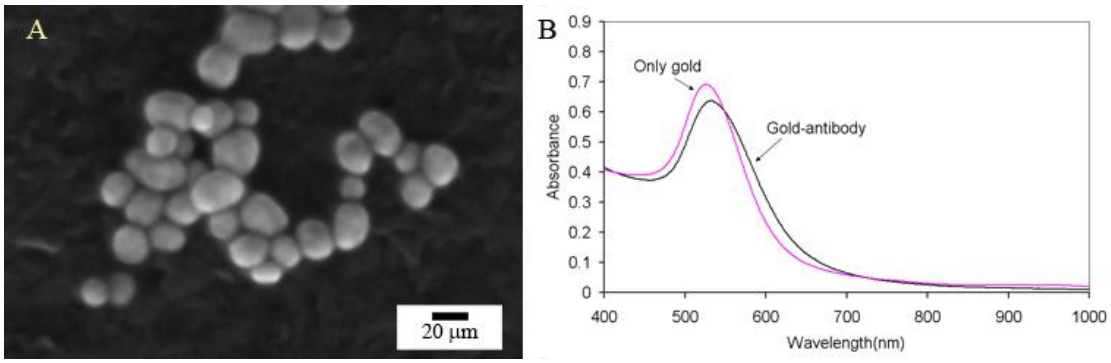

Figure S1. Characterization of gold nanospheres. (A) Unconjugated gold nanospheres taken using a scanning electron microscope. (B) Absorption spectra of conjugated and unconjugated gold nanospheres. Optical extinction of unconjugated gold nanospheres showing maximum extinction at ~526 nm but was slightly red-shifted to following conjugation with anti-*Toxoplasma gondii* antibody.

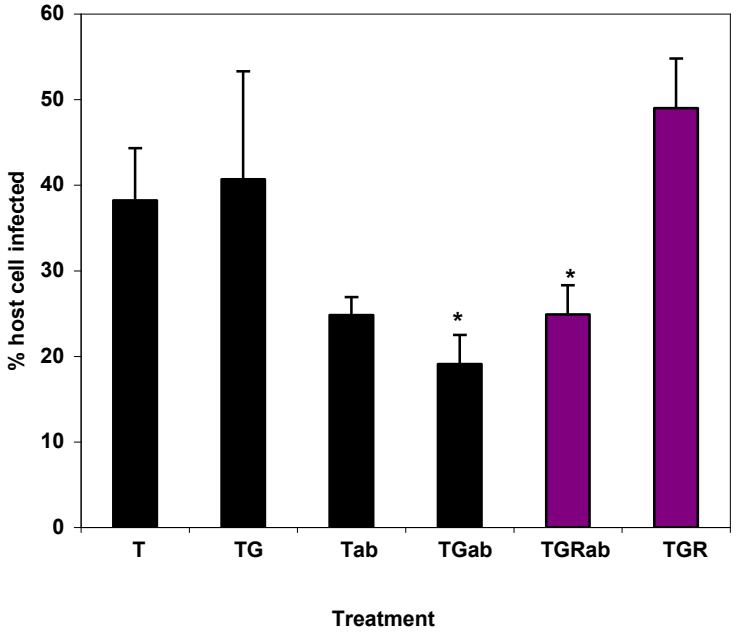

Figure S2. The effect of gold-anti *T. gondii* conjugates on invasion of host cells (CHO-K1 cells) by *T. gondii* tachyzoites. Each treatment lasted 1 hour. Significant inhibition of infection occurred when the tachyzoites were labelled with gold-anti *T. gondii* conjugates or anti *T. gondii* antibody alone compared with non-labelled tachyzoites and tachyzoites labelled with naked gold nanospheres at $P<0.05$. Key:

T= CHO-K1 infected with *T. gondii* tachyzoites only

TG= CHO-K1 infected with *T. gondii* tachyzoites pre-incubated with naked gold nanospheres

Tab= CHO-K1 infected with *T. gondii* tachyzoites pre-incubated with anti *T. gondii* antibody

TGab= CHO-K1 infected with *T. gondii* tachyzoites pre-incubated with gold-anti *T. gondii* conjugates

TGRab= CHO-K infected with *T. gondii* tachyzoites pre-incubated with gold nanorod-anti *T. gondii* conjugates

TGR= CHO-K infected with *T. gondii* tachyzoites pre-incubated with naked gold nanorods

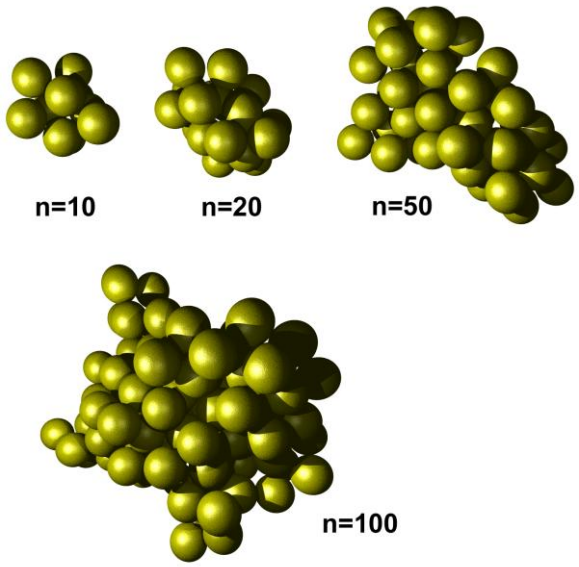

Figure S3. Randomly generated targets comprised of aggregated Au nanospheres of 15 nm diameter, with a 2 nm distance of closest approach. The surrounding medium is water.

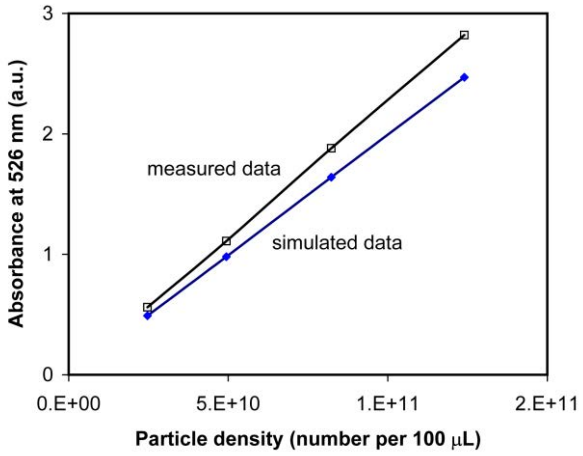

Figure S4. Standardised graph of absorbance ($-\log_{10}(I/I_0)$) as a function of concentration of gold nanoparticles per 100 μL. Also shown is a simulation of these concentrations of gold nanoparticles, performed using DDSCAT and the published bulk optical properties of gold. The Beer-Lambert Law was assumed to hold. In both cases a monodisperse population of 20 nm diameter gold spheres in water and a 1 cm optical path length was used or assumed.